

Mass spectra and transition magnetic moments of low lying charmed baryons in a quark model

Zahra Ghalenovi ^{*}and Masoumeh Moazzen Sorkhi
Department of Physics, Kosar University of Bojnord, Iran

February 21, 2022

Abstract

Excited state mass spectra of the low lying single charmed baryons with non strangeness have been calculated in a hypercentral approach. The six-dimensional hyperradial Schrödinger equation is solved by applying a simple variational method. We extend our scheme to predict the magnetic moments and the $\frac{3}{2}^+ \rightarrow \frac{1}{2}^+$ transition magnetic moments of Σ_c and Λ_c state baryons. A comparison of our results with the experimental data and predictions obtained in recent models is also presented.

Key words: Potential model, hyperspherical approach, perturbation theory, non-relativistic limit, transition magnetic moments.

1 Introduction

The $\Sigma_c(2455)$ and $\Lambda_c(2286)$ are the two lowest baryon states in the heavy flavor sector. Their descriptions and properties thus play a very important role in the understanding of strong interaction. Many theoretical models such as non-relativistic model [1, 2], relativistic quark model [3], Lattice QCD [4], QCD sum rule [5, 6, 7, 8], Quark-diquark model [9, 10, 11] and Faddeev approach [12] also have been presented to study the properties of heavy flavor baryons, however there are limited numbers of theoretical studies on the excited states and transition magnetic moments of heavy baryons. The purpose of this paper is to study the properties of non-strange single charm baryons. We calculate the ground and excited states mass spectra and magnetic moments of Σ_c and Λ_c baryons. We calculate the baryon spectrum in a two-step procedure: first, we introduce the perturbing hyperfine interaction and then obtain the baryon masses. We also compute the spin-orbit potential for the excited baryons. Second, we use the hypercentral model in order to solve the three-body Schrödinger equation by performing an variational method and obtain the wavefunction and eigenvalues of the baryon systems.

The measurement and calculation of electromagnetic transitions $B \rightarrow B'\gamma$ between $J = 3/2^+$ and $J = 1/2^+$ baryons is an important issue to understand the internal structure of baryons and observe new hadronic states experimentally. Here, we extend our scheme to calculate the $\frac{3}{2}^+ \rightarrow \frac{1}{2}^+$ transition magnetic moments of single charm baryons in a simple way. The paper is organized as follows. In Sec. 2 we introduce the hypercentral model. We present our potential model to solve the Schrödinger equation in Sec. 3. Our predictions for the baryon masses, magnetic moments and $\frac{3}{2}^+ \rightarrow \frac{1}{2}^+$ transition magnetic moments are presented in Sec. 4 and Sec. 5 includes conclusions.

^{*}z_ghalenovi@kub.ac.ir

2 The hypercentral constituent quark model

2.1 Hyperspherical coordinates

We consider the baryon system as a bound state of three constituent quarks. After removal of the center of mass coordinates, R , the configurations of three quarks can be described by the Jacobi coordinates, ρ and λ ,

$$\vec{\rho} = \frac{1}{\sqrt{2}}(\vec{r}_1 - \vec{r}_2), \quad \vec{\lambda} = \frac{1}{\sqrt{6}}(\vec{r}_1 + \vec{r}_2 - 2\vec{r}_3) \quad (1)$$

such that

$$m_\rho = \frac{2m_1m_2}{m_1 + m_2}, \quad m_\lambda = \frac{3m_3(m_1 + m_2)}{2(m_1 + m_2 + m_3)} \quad (2)$$

Here m_1 , m_2 and m_3 are the constituent quark masses. Instead of ρ and λ , one can introduce the hyperspherical coordinates, which are given by the angles $\Omega_\rho = (\theta_\rho, \phi_\rho)$ and $\Omega_\lambda = (\theta_\lambda, \phi_\lambda)$ together with the hyperradius x , and the hyperangle, ζ defined in terms of the absolute values of ρ and λ by

$$x = \sqrt{\rho^2 + \lambda^2}, \quad \xi = \arctan\left(\sqrt{\frac{\rho}{\lambda}}\right) \quad (3)$$

Therefore the Hamiltonian will be

$$H = \frac{p_\rho^2}{2m} + \frac{p_\lambda^2}{2m} + V(x). \quad (4)$$

In hyperspherical coordinates the Laplace operator for three-body system is written as follows:

$$\nabla^2 = (\nabla_\rho^2 + \nabla_\lambda^2) = -\left(\frac{d^2}{dx^2} + \frac{5}{x} \frac{d}{dx} - \frac{L^2(\Omega_\rho, \Omega_\lambda, \xi)}{x^2}\right), \quad (5)$$

Therefore the kinetic energy operator of a three-body problem can be written as ($\hbar = c = 1$):

$$-\frac{1}{2m}(\nabla_\rho^2 + \nabla_\lambda^2) = -\frac{1}{2m}\left(\frac{d^2}{dx^2} + \frac{5}{x} \frac{d}{dx} - \frac{L^2(\Omega_\rho, \Omega_\lambda, \xi)}{x^2}\right). \quad (6)$$

The eigenfuctions of the grand angular operator $L^2(\Omega)$ are the so called hyperspherical harmonics

$$L^2(\Omega_\rho, \Omega_\lambda, \xi)Y_{[\gamma], l_\rho, l_\lambda}(\Omega_\rho, \Omega_\lambda, \xi) = \gamma(\gamma + 1)Y_{[\gamma], l_\rho, l_\lambda}(\Omega_\rho, \Omega_\lambda, \xi). \quad (7)$$

Where γ is the grand angular quantum number given by $\gamma = 2n + l_\rho + l_\lambda$; l_ρ and l_λ are the angular momenta corresponding to the Jacobi coordinates ρ and λ and n is a non-negative integer number.

In the hypercentral approach, the three-quark interaction is assumed to be hypercentral, that is the energy of the system depends only on the quarks distance

$$V_{3q}(\rho, \lambda) = V(x), \quad (8)$$

as a consequence, the three-quark wave function is factorized

$$\psi_{3q}(\rho, \lambda) = \psi_{\nu, \gamma}(x)Y_{[\gamma], l_\rho, l_\lambda}(\Omega_\rho, \Omega_\lambda, \xi). \quad (9)$$

where ν determines the number of the nodes of the wave function. The hyperradial wave fuction $\psi_{\nu, \gamma}(x)$ is obtained as a solution of the hyperradial equation

$$\left[\frac{d^2}{dx^2} + \frac{5}{x} \frac{d}{dx} - \frac{\gamma(\gamma + 4)}{x^2}\right]\psi_{\nu, \gamma}(x) = -2m[E_{\nu, \gamma} - V(x)]\psi_{\nu, \gamma}(x). \quad (10)$$

2.2 Potential model

To make a phenomenological model, we should introduce a potential model such that the QCD concepts of the quark-quark interactions be satisfied. From the experimental observations, we find that all hadrons are made of quarks and no single quark can be individually observed. This fact imply that the quarks are confined in hadrons in the vacuum. According to quantum chromodynamics, there are super-strong color attractive interactions among the quarks, causing three quarks of different colors to be confined together and form a colorless baryon. Moreover the experimental baryon spectroscopy shows an underlying SU(6) symmetry. Therefore an interaction potential should contain two main terms: a confining SU(6) invariant term, and a SU(6) breaking term describing the splitting of multiplets of baryons. Thus the three-quark interaction can be generally written in the form of

$$V_{3q} = V_{SU(6)-invariant} + V_{SU(6)-breaking} + V_{Spin-Orbit}. \quad (11)$$

for the $V_{SU(6)-invariant}$ sector, the Coulomb-plus-linear potential $(-\frac{\tau}{x} + \beta x)$, known as the Cornell potential, has received a great deal of attention both in particle and atomic physics. Our potential model is a combination of lattice QCD calculations plus the Isgur-Karl interaction [13, 14]. Our potential includes the short distance Coulombic interaction of quarks and the large distance quark confinement via the linear terms in a simple form. Coulombic term alone is not sufficient because it would allow free quarks to ionize from the system. The nonperturbative SU(6)-invariant part is introduced as follows:

$$V_{SU(6)-invariant} = -\frac{\tau}{x} + \beta x \quad (12)$$

where x is the hyper radius and τ and β are constant. The perturbative interactions are considered as a combination of SU(6)-breaking and spin-orbit interaction terms. The spin-orbit interaction is introduced as

$$V_{Spin-Orbit} = V_{\gamma s}(\vec{\gamma} \cdot \vec{S}) \quad (13)$$

where

$$V_{\gamma s}(x) = \frac{1}{2m_i m_j x} [3 \frac{dV_V}{dx} - \frac{dV_S}{dx}]. \quad (14)$$

V_V and V_S are the coulombic and confining parts of Eq. 12 respectively, and m_i and m_j are the masses of i th and j th quarks. The SU(6)-breaking part of the interactions is considered as follows:

$$V_{SU(6)-breaking} = V_{Spin} + V_{Isospin}. \quad (15)$$

We make the following model for spin-spin and isospin-isospin interaction

$$V_{Spin} = \frac{A_S}{6m_\rho m_\lambda} \frac{e^{-\frac{x}{x_0 S}}}{xx_0^2} \Sigma_{i < j} (\vec{s}_i \cdot \vec{s}_j), \quad (16)$$

and

$$V_{Isospin} = \frac{A_I}{6m_\rho m_\lambda} \frac{e^{-\frac{x}{x_0 I}}}{xx_0^2} \Sigma_{i < j} (\vec{t}_i \cdot \vec{t}_j), \quad (17)$$

where \vec{s}_i and \vec{t}_i the spin and isospin operators of the i th quark respectively and A and x_0 are constants. Then from Eqs. (13-17), the hyperfine interaction is given by

$$V_{hyp} = V_{Spin} + V_{Isospin} + V_{spin-Orbit}. \quad (18)$$

The contributions of this hyperfine interaction is added to the unperturbed SU(6)-invariant energies provided by the potential 12. In the next section, we obtain the wave function and energy of the system in the framework of a simple approximation with confining potential 12.

2.3 Solution of Schrödinger equation

The equation 10 can be solved analytically for the hyperCoulomb potential

$$V_{hc} = -\frac{\tau}{x}. \quad (19)$$

The eigenvalues of the hyperCoulomb problem can be obtained by generalizing to six dimensions. The calculations performed in three dimensions, obtaining

$$E_{n,\gamma} = -\frac{\tau^2 m}{2n^2} \quad (20)$$

where $n = \gamma + \frac{5}{2} + \nu$ is the principal quantum number and $\nu = 0, 1, 2, \dots$ is the radial quantum number that counts the number of nodes of the wave function.

The eigenfunctions of 10 with the hyperCoulomb potential can be obtained analytically and are [15]

$$\psi_{\nu,\gamma}(x) = \left[\frac{\nu!(2g)^6}{(2\gamma + 2\nu + 5)(2\gamma + \nu + 4)!} \right]^{\frac{1}{2}} (2gx)^\gamma e^{-gx} L_\nu^{2\gamma+4}(2gx) \quad (21)$$

where $g = \frac{m\tau}{\gamma + \nu + 5/2}$ and $L_\nu^{2\gamma+4}(2gx)$ are the Laguerre polynomials. We have plotted the distribution of the hyperradial wave function density for the ground and first radial excited states of the qqc state baryons in fig. 1.

The hyperCoulomb potential does not confine quarks in hadrons and therefore we add the linear confining potential to the hyperCoulomb interaction 19 and therefore the potential we use is in the form of the equation 12. The equation can not be solved analytically with potential 12, except when the linear term is treated as a perturbation. Here, we consider this situation and using the obtained wave function 21 we can obtain the expectation values of the linear term for different baryon states. Therefore the energy eigenvalues for the baryons are obtained as

$$E_{n,\gamma} = -\frac{\tau^2 m}{2n^2} + \frac{\beta}{2m\tau} [3n^2 - \gamma(\gamma + 4) - \frac{15}{4}] \quad (22)$$

which is valid, to a good approximation, for the low lying states.

3 The spectrum and electromagnetic transitions

Using the obtained energy eigenvalues 22 and wave function 21 one can calculate the baryon mass by sum of the quark masses, energy eigenvalues and the hyperfine interaction potential treated as a perturbation:

$$M_{baryon} = \sum_{i=1}^3 m_i - \frac{\tau^2 m}{2n^2} + \frac{\beta}{2m\tau} [3n^2 - \gamma(\gamma + 4) - \frac{15}{4}] + \langle H_{hyp} \rangle \quad (23)$$

where using the unperturbed wave function 21 we can obtain the perturbative hyperfine interaction $\langle H_{hyp} \rangle$. The parameters used in our model (listed in table 1) are obtained from our previous work [16] in which we have studied the light baryon resonances in a quark model. We use the experimental mass of $\Xi_{cc}(3520)$ baryon to determine the mass of the charm quark. The value of A_I is also fitted to the mass difference between $\Sigma_c(2455)$ and $\Lambda_c(2286)$ states.

Our predictions for single charm baryon spectra are listed in tables 2-3 and compared with the experimental data [17, 18] or other theoretical predictions [19, 20, 21, 22, 23]. For Λ_c^+ state, as the first discovered singly charmed baryon, our results are in good agreement with those of other works. The experimental known ground state is $\Lambda_c(2286)^+$ and the first orbital excited states are $\Lambda_c(2595)^+$ and $\Lambda_c(2625)^+$ with quantum numbers $J = 1/2^-$ and $J = 3/2^-$ respectively. $\Lambda_c(2765)^+$ was also observed

by CLEO collaboration [18] but its quantum number is still unknown. Our predictions indicate that $\Lambda_c(2765)^+$ can be considered as the first radial excited state of $\Lambda_c(2286)^+$ with $J^P = 1/2^+$ which is in good agreement with other predictions [19, 20, 22, 23]. $\Lambda_c(2880)^+$ with $J = 5/2^+$ is also known and our results show it can be considered as the second orbital excited state of $\Lambda_c(2286)^+$ in favor of Refs. [19, 20, 22].

For Σ_c , two ground states $\Sigma_c(2455)$ and $\Sigma_c(2520)$ with J^P values $J = \frac{1}{2}^+$ and $J = \frac{3}{2}^+$ has reported by Ref. [17]. $\Sigma_c(2800)$ is also found but its quantum number is still unknown. Refs. [19, 20] have predicted that as $1P$ state. Our results listed in table 3 indicate that we can consider $\Sigma_c(2800)$ as $1P$ state with a mass difference of 62 MeV to the experimental mass 2806 MeV . Our results show that $2S$ state is also a good candidate for $\Sigma_c(2800)$.

Within the baryons the mass of the quarks may get modified due to its binding interactions with the other two quarks. The effective quark mass is defined as

$$m_i^{eff} = m_i \left(1 + \frac{E_{n,\gamma} + \langle H_{hyp} \rangle}{\sum_i m_i} \right) \quad (24)$$

Such that the mass of the baryon is

$$M_{baryon} = \sum_i m_i^{eff} \quad (25)$$

The magnetic moment of baryon is obtained in terms of the spin-flavour wave function of the constituent quarks as

$$\mu_B = \sum_i \langle \phi_{sf} | \mu_i \vec{\sigma}_i | \phi_{sf} \rangle \quad (26)$$

where $\mu_i = \frac{e_i}{2m_i^{eff}}$. Here, e_i and $s_i = \frac{\sigma_i}{2}$ represent the charge and the spin of the quark constituting the baryonic state and $|\phi_{sf}\rangle$ represents the spin-flavour wave function of the respective baryonic state. The magnetic moments of charm baryons obtained in our model are listed in table 4 and compared with other predictions [24, 25, 26, 27, 28]. The present calculations are in very good agreement with those of Ref. [27] and our previous work [26].

We can obtain the magnetic moments of different transitions by sandwiching $\sum_i \mu_i \vec{\sigma}_i$ between the appropriate $3/2^+$ and $1/2^+$ baryon wave functions. The transition magnetic moments for $\frac{3}{2}^+ \rightarrow \frac{1}{2}^+$ are computed as [29, 30]

$$\mu_{\frac{3}{2}^+ \rightarrow \frac{1}{2}^+} = \sum_i \langle \phi_{sf}^{\frac{3}{2}^+} | \mu_i \sigma_i | \phi_{sf}^{\frac{1}{2}^+} \rangle. \quad (27)$$

In order to evaluate $B_{3/2} \rightarrow B_{1/2} \gamma$ transition magnetic moments, we take the geometric mean of effective quark masses of the constituent quarks of initial- and final-state baryons:

$$m^{eff} = \sqrt{m_{i(\frac{3}{2}^+)}^{eff} m_{i(\frac{1}{2}^+)}^{eff}} \quad (28)$$

where m_i^{eff} is the effective quark mass of the i th quark inside the corresponding baryon.

Our results for the transition magnetic moments are listed in table 5 and compared with other results [25, 31, 32, 33]. Our predictions are very close to those obtained by Ref. [31].

4 Conclusions

In this paper we have investigated the non-strange charm baryons by employing the hyperspherical formalism with a color Coulomb plus linear confining potential. Using the theory of time-independent perturbation for the hyperfine interactions, we got the effects of spin, isospin and spin-orbit potentials in the shift of baryon energy. We have considered the color Coulomb part as parent and the linear term as a perturbation. This method is valid, to a good approximation, for the low lying state baryons. Using the hyperCoulomb wave function we could obtain the mass spectra and transition magnetic moments of single charm baryons. Our results are in good agreement with those of other works.

5 Acknowledgments

This work was supported by Kosar University of Bojnord with the Grant number (No. 9809141444).

References

- [1] Z. Shah and A. Kumar Rai, Chin. Phys. C **42**, 5 (2018).
- [2] Z. Ghaleyni et al., Chin. J. Phys. **51**, 6 (2013).
- [3] D. Ebert, R. N. Faustov and V. O. Galkin, Phys. Rev. D **84**, 014025 (2011).
- [4] N. Mathur, R. Lewis, and R. M. Woloshyn, Phys. Rev. D **66**, 014502 (2002).
- [5] Q. Mao, H. X. Chen, W. Chen, A. Hosaka, et al., Phys. Rev. D **92**, 114007 (2015).
- [6] Liu et al., Phys. Rev. D **77**, 014031 (2008).
- [7] T. M. Aliev, K. Azizi, A. Ozpineci, Nucl. Phys. B **808**, 137(2009).
- [8] T. M. Aliev, K. Azizi, and A. Ozpineci, Phys. Rev. D **79**, 056005 (2009).
- [9] D. Ebert, R. N. Faustov, and V. O. Galkin, Phys. Rev. D **72**, 034026 (2005).
- [10] K. Thakkar, A. Majethiya and P. C. Vinodlumar, Eur. Phys. J. Plus **131**, 339 (2016).
- [11] A. Majethiya, K. Thakkar and P. C. Vinodlumar, Chin. J. Phys. **54**, 495 (2016).
- [12] S. M. Gerasyuta, and D. V. Ivanov, Nuovo Cimento A **112**, 261 (1999).
- [13] N. Isgur and Karl, Phys. Rev. D **19**, 2653 (1978).
- [14] N. Isgur and G. Karl, Phys. Rev. D **18**, 4187 (1978).
- [15] E. Santopinto, F. Iachello and M. M. Gainini, Eur Phys. J. A **1**, 307 (1998).
- [16] Z. Ghaleyni and M. Moazzen Sorkhi, Int. J. Mod. Phys. E **26**, 7 (2017).
- [17] M. Tanaboshi et al (Particle Data Group), Phys. Rev. D **98**, 030001 (2018).
- [18] M. Artiro et al (CLEO collaboration), Phys. Rev. Lett. **86**, 4479 (2001).
- [19] Z. Shah, K. Thakkar, A. Kumar Rai and P. C. Vindokumar, Chin. Phys. C **12**, 123102 (2016).
- [20] D. Ebert, R. N. Faustov, and V. O. Galkin, Phys. Rev. D **84**, 014025 (2011).
- [21] T. Yoshida, E. Hiyama, A. Hosaka, M. Oka, and K. Sadato, Phys. Rev. D **92**, 114029 (2015).

- [22] B. Chen, K. W. Wei, and A. Zhang, Eur. Phys. J. A **51**, 82 (2015).
- [23] Y. Yamaguchi, S. Ohkoda, A. Hosaka, T. Hyodo, and S. Yasui, Phys. Rev. D **91**, 034034 (2015).
- [24] B. Patel, A. Kumar Rai and P.C. Vinodkumar, J. Phys. G: Nucl. Part. Phys. **35**, 065001 (2008).
- [25] N. Sharma, B. Dahiya, P.K. Chately and M. Gupta, Phys. Rev. D **81**, 073001 (2010).
- [26] Z. Ghalenovi, A.A. Rajabi, S. Qin and D.H. Rischke, Mod. Phys. Lett. A **29**, 20 (2014).
- [27] S. Kumar, R. Dhir and R.C. Verma, J. Phys. G: Nucl. Part. Phys. **31**, 141 (2005).
- [28] A. Faessler et al., Phys. Rev. D **73**, 094013 (2006).
- [29] Z. Ghalenovi, Int. J. Theor. Phys. **57**, 9 (2018).
- [30] Z. Ghalenovi and M. Mozzaen Sorkhi, Eur. Phys. J. Plus **133**, 301 (2018).
- [31] R. Dhir and R.C. Verma, Eur. Phys. J. A **42**, 243 (2009).
- [32] A. Bernatos and V. Simonis, Phys. Rev. D **87**, 074016 (2013).
- [33] T. M. Aliev, K. Azizi, and A. Ozpineci, Phys. Rev. D **79**, 056005 (2009).

Table 1: Quark-model parameters

m_q	313 MeV
m_c	1747 MeV
β	0.87 fm^{-1}
τ	2.54
A_S	67.4
x_{0S}	1.93 fm
A_I	390.2
x_{0I}	1.87 fm

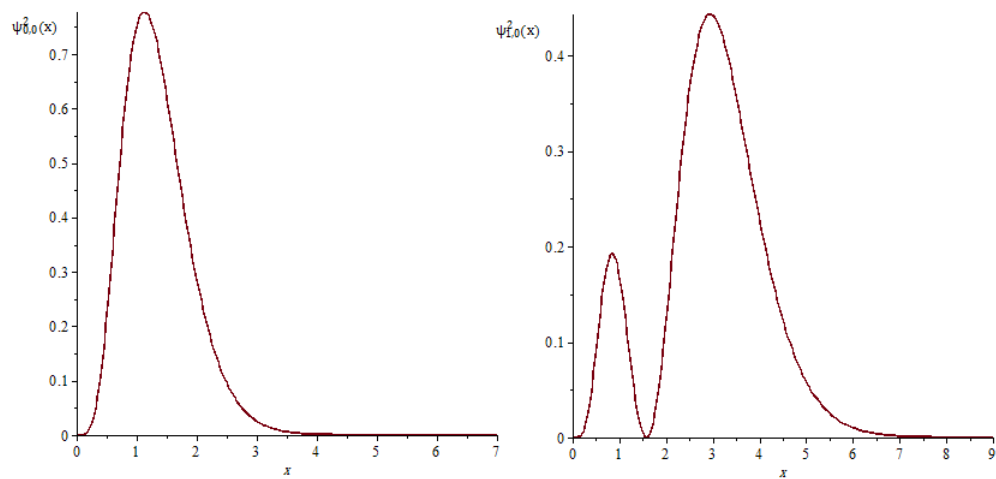


Figure 1: $\psi_{\nu,\gamma}^2$ for the ground state (left) and first radial excited state (right) vs. x .

Table 2: Mass spectra of Λ_c^+ baryon (in MeV).

$n^{2S+1}L_J$	Our	Exp	Ref.[19]	Ref.[20]	Ref.[22]	Ref.[23]
$1^2S_{\frac{1}{2}}$	2285	2286.46 ± 0.14	2287	2286	2286	2268
$2^2S_{\frac{1}{2}}$	2740	2766 ± 2.4	2758	2769	2766	2791
$3^2S_{\frac{1}{2}}$	3176		3134	3130	3112	2983
$4^2S_{\frac{1}{2}}$	3672		3477	3430	3397	3154
$1^2P_{\frac{1}{2}}$	2693	2592.25 ± 0.28	2694	2589	2591	2625
$1^2P_{\frac{3}{2}}$	2651	2628.11 ± 0.19	2640	2627	2629	2830
$2^2P_{\frac{1}{2}}$	3115		3062	2983	2989	
$2^2P_{\frac{3}{2}}$	3093		3015	3005	3000	
$3^2P_{\frac{1}{2}}$	3598		3397	3303	3296	
$3^2P_{\frac{3}{2}}$	3591		3354	3222	3301	
$1^2D_{\frac{3}{2}}$	2997		2924	2874	2857	3120
$1^2D_{\frac{5}{2}}$	2986	2881.63 ± 0.24	2854	2880	2879	3125
$2^2D_{\frac{3}{2}}$	3495		3263	3189	3188	3194
$2^2D_{\frac{5}{2}}$	3483		3204	3209	3198	3194
$1^2F_{\frac{5}{2}}$	3358		3130	3097	3075	3092
$1^2F_{\frac{7}{2}}$	3344		3052	3078	3092	3128

Table 3: Mass spectra of Σ_c^0 baryon (in MeV).

$n^{2S+1}L_J$	Our	Exp	Ref.[19]	Ref.[20]	Ref.[21]	Ref.[23]
$1^2S_{\frac{1}{2}}$	2452	2453.75 ± 0.14	2452	2443	2460	2455
$2^2S_{\frac{1}{2}}$	2801		2891	2901	3029	2958
$3^2S_{\frac{1}{2}}$	3202		3261	3271	3171	3115
$4^2S_{\frac{1}{2}}$	3685		3593	3581		
$1^4S_{\frac{3}{2}}$	2510	2518.48 ± 0.2	2518	2519	2523	2519
$2^4S_{\frac{3}{2}}$	2815		2917	2936	3065	2995
$3^4S_{\frac{3}{2}}$	3210		3274	3293	3094	3116
$4^4S_{\frac{3}{2}}$	3689		3601	3598		
$1^2P_{\frac{1}{2}}$	2744	2806^{+5}_{-7}	2809	2799	2802	2848
$1^2P_{\frac{3}{2}}$	2702		2755	2798	2807	2763
$1^4P_{\frac{1}{2}}$	2803		2835	2713		
$1^4P_{\frac{3}{2}}$	2761		2782	2773		
$1^4P_{\frac{5}{2}}$	2691		2710	2789	2839	2790
$2^2P_{\frac{1}{2}}$	3136		3174	3172	2826	
$2^2P_{\frac{3}{2}}$	3115		3128	3172	2837	
$2^4P_{\frac{1}{2}}$	3164		3196	3125		
$2^4P_{\frac{3}{2}}$	3143		3151	3151		
$2^4P_{\frac{5}{2}}$	3108		3090	3161	3316	
$3^2P_{\frac{1}{2}}$	3615		3505	3488	2909	
$3^2P_{\frac{3}{2}}$	3602		3465	3486	2910	
$3^4P_{\frac{1}{2}}$	3631		3525	3455		
$3^4P_{\frac{3}{2}}$	3618		3485	3469		
$3^4P_{\frac{5}{2}}$	3597		3433	3475	3521	
$1^2D_{\frac{3}{2}}$	3023		3112	3043		3095
$1^2D_{\frac{5}{2}}$	3003		2993	3038	3099	3003
$1^4D_{\frac{1}{2}}$	3054		3036	3041		
$1^4D_{\frac{3}{2}}$	3041		3061	3040		
$1^4D_{\frac{5}{2}}$	3020		2968	3023		
$1^4D_{\frac{7}{2}}$	2991		2909	3013		3015
$2^2D_{\frac{3}{2}}$	3512		3398	3366		
$2^2D_{\frac{5}{2}}$	3504		3316	3365	3114	
$2^4D_{\frac{1}{2}}$	3522		3376	3370		
$2^4D_{\frac{3}{2}}$	3515		3442	3364		
$2^4D_{\frac{5}{2}}$	3499		3339	3349		
$2^4D_{\frac{7}{2}}$	3484		3265	3342		
$1^2F_{\frac{7}{2}}$	3363		3245	3283		
$1^2F_{\frac{9}{2}}$	3349		3165	3227		
$1^4F_{\frac{3}{2}}$	3380		3332	3288		
$1^4F_{\frac{5}{2}}$	3370		3268	3254		
$1^4F_{\frac{7}{2}}$	3356		3189	3253		
$1^4F_{\frac{9}{2}}$	3338		3094	3209		

Table 4: Magnetic moments of the ground states of Σ_c and Λ_c^0 baryons in terms of μ_N .

Baryon	μ_B	Prediction	Ref. [24]	Ref. [25]	Ref. [26]	Ref. [27]	Ref. [28]
Λ_c^+	μ_c	0.37	0.38	0.392		0.37	0.37
Σ_c^{++}	$\frac{4}{3}\mu_u - \frac{1}{3}\mu_c$	2.45	2.27	2.20		2.36	1.86
Σ_c^+	$\frac{2}{3}\mu_u + \frac{2}{3}\mu_d - \frac{1}{3}\mu_c$	0.52	0.50	0.30		0.62	0.37
Σ_c^0	$\frac{4}{3}\mu_d - \frac{1}{3}\mu_c$	-1.39	-1.01	-1.60		-1.36	-1.11
Σ_c^{*++}	$2\mu_u + \mu_c$	4.10	3.84	3.92	4.10		
Σ_c^{*+}	$\mu_u + \mu_d + \mu_c$	1.27	1.25	0.97	1.32		
Σ_c^{*0}	$2\mu_d + \mu_c$	-1.54	-0.84	-1.99	-1.44		

Table 5: Transition Magnetic moments ($|\mu_{\frac{3}{2}^+ \rightarrow \frac{1}{2}^+}|$) of single charm baryons in μ_N .

Decay Mode	$\mu_{B \rightarrow B' \gamma}$	Our	Ref. [25]	Ref. [31]	Ref. [32]	Ref. [33]
$\Sigma_c^{*++} \rightarrow \Sigma_c^{++} \gamma$	$\frac{2\sqrt{2}}{3}(\mu_u - \mu_c)$	1.47	1.37	1.41	0.90	1.33 ± 0.38
$\Sigma_c^{*+} \rightarrow \Sigma_c^+ \gamma$	$\frac{\sqrt{2}}{3}(\mu_u + \mu_d - 2\mu_c)$	0.12	0.003	0.09	0.06	0.57 ± 0.09
$\Sigma_c^{*0} \rightarrow \Sigma_c^0 \gamma$	$\frac{2\sqrt{2}}{3}(\mu_d - \mu_c)$	1.21	2.40	1.22	1.03	0.24 ± 0.05
$\Sigma_c^{*+} \rightarrow \Lambda_c^+ \gamma$	$\frac{\sqrt{2}}{\sqrt{3}}(\mu_u - \mu_d)$	2.41	1.48	2.28	1.70	2.00 ± 0.53